



J. Serb. Chem. Soc. 89 (5) 679–692 (2024)
JSCS–5748

Influence of the elasticity variation of the 3D printed PMMA structure on the axial tooth vibration

LIVIJA CVETICANIN^{1,2*}, MILJANA PRICA¹ and SANJA VUJKOV³

¹University of Novi Sad, Faculty of Technical Sciences, Novi Sad, Serbia, ²Obuda University, Budapest, Hungary and ³University of Novi Sad, Faculty of Medicine, Department of Dentistry, Novi Sad, Serbia

(Received 18 January, revised 15 February, accepted 7 March 2024)

Abstract: Recently, 3D printing with poly methyl methacrylate (PMMA) has been widely used in dentistry: 3D printing is a suitable method for producing any complex three-dimensional shape, and PMMA is a material that has suitable properties in the oral cavity environment. That is why 3D printing is very often used to make PMMA teeth. There is the impact between teeth during chewing that causes shape variation and tooth vibration. As cyclic vibrations adversely affect the durability of PMMA teeth, they must be eliminated. The object of this work is to study the axial vibrations of a 3D printed tooth, as well as to give recommendations for modifying the PMMA structure with the aim of vibration damping. Tooth vibration is mathematically modeled and analytically solved. The obtained result provides a link between the vibrational properties and the elasticity variation of the PMMA material. The function that defines the change in elasticity of PMMA depends on the “slow time”. (The term “slow time” implies a product of time and a parameter that is less than one). For a decreasing elasticity function, the vibration is of damped type: for higher is the elasticity reduction, the faster is the vibration decay. Based on the determined elasticity function, the modification of the PMMA structure can be realized. Authors propose the application of the obtained elasticity variation function for programming 4D printing with modified PMMA.

Keywords: 3D printing; PMMA in dentistry; variable modulus of elasticity; axial vibration in tooth; analytic solving method; planning of 4D printing.

INTRODUCTION

In modern dentistry, new technologies and especially new materials are the drivers of development. One of the new techniques for making complex shaped three-dimensional objects in dentistry, like teeth, bridges, implants, bone supplements, *etc.*, is the so-called 3D printing. It is the procedure for fabrication of a

* Corresponding author. E-mail: cveticanin@uns.ac.rs
<https://doi.org/10.2298/JSC240118029C>

three-dimensional object based on the 3D CAD or digital model. During the process of creating an object with 3D printing, under computer control, “layer by layer” of material is applied until the final structure is formed. The advantages of digital manufacturing is speed and efficiency. For 3D printing the so called “3D printing materials” are applied. There is the special technology on a 3D printer which produces the material from chemical components that enter into a chemical reaction under the influence of liquid, heat, radiation, *etc.* In dentistry, it is important the material to be close to those of living beings or most acceptable for the human body. In the last ten years materials for 3D printing attract research interest.

In general, materials applied in dentistry can be classified into 4 groups: polymers, metals, ceramics and biomaterials.¹ By comparing the 4 materials it is found that the chemical and physical properties of polymers are better than those of ceramics and metals. Polymers have advantage due to elasticity and tensile strength which provide high performance and durability feature and are applied for denture bases, artificial teeth, temporary crowns, bridge and crown facings and implants.² Polymers are used in polymeric resins for replacing tooth structure and missing tooth. Advantage of these resins is their ability to bond with other resins directly to the tooth structure. According to these founding the 3D printing material is usually assumed to be of polymer type. Synthetic and natural bio polymers are applied in 3D printing.³ The applied synthetic polymers are: poly capro-lactone (PCL), polymethyl methacrylate (PMMA), polylactic acid (PLA), acrylonitrile butadiene styrene (ABS), polyvinyl alcohol (PVA), polylactic-co-glycolic acid (PLGA) and ultraviolet (UV) resins. The following three natural biopolymers are also used: hyaluronic acid (HA), chitosan and alginate. However, one of the most often used polymers in dentistry which support long-term dental applications is the PMMA.^{4,5}

Chemical construction and property definition

PMMA (IUPAC name: poly(methyl 2-methylpropenoate)) is a synthetic polymer prepared by the free radical addition and polymerization of methyl methacrylate ($C_5O_2H_8$) to polymethyl methacrylate ($C_5O_2H_8$)_n. The polymerization reaction is initiated and activated by generating a free radical either chemically or with energy (such as heat, light, microwaves). In the propagation stage, the activated polymerization continues *via* the binding of monomers followed by termination through shifting of the free electrons to the chain end. The majority of PMMA are supplied as polymeric powders and monomer liquids.

The basic component of the liquid is the methyl methacrylate (MMA), the methyl ester of methyl 2-methylpropenoate. In this colorless liquid an accelerator, inhibitor, plasticizer, as cross-linking agent are added. MMA is the highest-volume compound among lower methacrylates used for polymer synthesis.

Unlike acrylic acid (AA), MAA and its alkyl esters have a methyl group adjacent to the double bond in the acyl component, hindering nucleophile addition at this site. This nucleophile addition is correlated with decreased cytotoxicity and genotoxicity of methacrylates compared to the acrylates. The powder consists of acrylic or copolymer heads, an initiator (benzoyl peroxide pigments – mercury sulfide, cadmium sulfide or dyes), opacifiers (titanium dioxide) and in addition – dyed synthetic fibers, plasticizers, inorganic particles (glass fibers, zirconium silicate).

To avoid any discrepancies, it is necessary to use the recommended ratio of PMMA powder and liquid (2.5:1 or 3–3.5:1, volume ratio). In the case of a high powder-to-liquid ratio, this means that not all of the PMMA beads will be wet, leading to a granular texture, while a low powder-to-liquid ratio.

In 3D printing the exothermic chemical reaction starts upon mixing of the PMMA powder and liquid, which harden either chemically (cold cure) or *via* energy application in the case of heat-cured PMMA materials.⁶ The phases of process of PMMA polymerization are initiation, activation, propagations and termination.

Finally, although numerous new alloplastic materials show promise, the versatility and reliability of PMMA cause it to remain a popular and frequently used material.⁷ The main advantage of the PMMA material is its long durability, low cost and high performance. In addition the material is non-toxic, biocompatible, inert, and has no color change in time. Due to these characteristics PMMA is material for temporary crowns and bridges, artificial teeth, implants, to manufacture surgical guides, custom trays, working casts and temporary restorations.⁸

Comparison of PMMA produced with 3D printing with CAD/CAM milling and conventional procedure

In dentistry the PMMA parts are made with 3D printing, computer-aided designing/computer-aided manufacturing (CAD/CAM) milling or with conventional procedure. For comparing the mentioned methods, let us consider the physical and mechanical properties of a PMMA provisional crown produced using the previously mentioned three procedures.⁹ The following mechanical characteristics were compared: fracture strength, flexural strength, elastic modulus, toughness, peak strain, resilience, micro-hardness, surface roughness, wear resistance, and also the following physical properties: color change, water sorption and solubility. It is found that the fracture strength, flexural strength, peak stress, elastic modulus, and wear resistance are some of the mechanical properties better for 3D printed PMMA structure compared to other two ones. However, it was not the case for toughness, resilience, and micro-hardness. In addition, 3D printed PMMA provisional crown had inferior physical properties. In spite of disadvantages, the 3D printed PMMA structure was suggested to be

used as an alternative to conventional and CAD/CAM milled materials.⁹ Namely, 3D printing made available a number of PMMA dental models to be easily fabricated, polished and repaired using the 3D printers. 3D printers reduce the production time and allow the production of multiple 3D copies.¹⁰ In addition, the 3D printing available the production of any shape due to the fact that three-dimensionally printed materials are fabricated by a layering technique. Conventional fabrication using PMMA with a mixture of self-polymerising powder and liquid requires longer cure times than it is in 3D printing. However, the disadvantages of 3D printing PMMA require to be investigated and eliminated.¹¹

Mechanical and physical properties of PMMA in dentistry

Measurements done on the 3D printed PMMA parts revealed that the tensile strength is 2.91 MPa and a modulus of elasticity of 223 MPa.¹² Comparing the values with those obtained for the same parts produced by traditional methods show that the first are worse. It was the reason to develop methods to improve properties of 3D printed parts in dentistry and they are as follows:

1. To improve the mechanical properties in 3D printed PMMA the thickness of layers during the printing process has to be controlled: the lower the layer thickness of printing the more layer-to-layer interfaces will be available; thus, each layer will be polymerized in a better way, which will increase the mechanical properties of these materials. The materials display superior mechanical properties if the build orientation for layers is deposited perpendicular to the direction of the applied load.

2. Improvement of mechanical properties in 3D printing is possible by infiltration of epoxy and smaller particles which may influence the qualities of the final products. To obtain better dimensional accuracy and resiliency, but also longer term application PMMA has to be mixed with some additional components. Modifications of PMMA involving chemical or mechanical reinforcement using supplementary materials (fibers, nanofillers, nanotubes and hybrid materials) have resulted in remarkable improvements in the mechanical (impact strength, cyclic fatigue, flexural strength, and wear resistance), physical (thermal conductivity, water sorption, solubility and dimensional stability), and biological (antimicrobial activity, biocompatibility) properties.⁶ Nanodiamonds in low concentrations can be added as reinforcement to improve the overall properties of PMMA-based fixed interim prostheses.¹³ The tensile strength is up to 26.6 MPa and the modulus of elasticity is 1184 MPa. Increasing the content of nanodiamonds the modulus of elasticity reaches its highest value of 2084 MPa. PMMA composites printed with three different reinforcements: aluminum nitride, titanium oxide and barium titanate have the tensile strength even 3200–4000 MPa¹⁴ and elastic modulus of 1075 MPa.¹⁵

3. After fabrication, 3D-printed materials may be subjected to post-treatments, which would increase the degree of conversion and lead to lower residual monomers and increased mechanical properties. To improve physical and mechanical properties such as density, elasticity and strength of material the polymerization process through heat and press has to be applied. It gives the PMMA material to be dimensionally stable but chemically unstable in the oral cavity and is sensitive on water sorption or dehydration.⁶ The conclusion is that the post-treatment of PMMA for dental application is not recommended.

During chewing process each tooth is dynamically loaded with the impact force acting along the tooth's vertical axis. The force causes tooth deformation which is extreme small, as the property of natural tooth material is rigid. As previously mentioned, the PMMA material, which is suggested for tooth substitution, has certain elastic property differing from that of the natural tooth. During each chewing the PMMA tooth undergoes some deformation and shape variation which is periodically repeated. The impact force in chewing causes axial vibration in the elastic 3D printed PMMA tooth. This vibration is unwilling as it dissipate the useful chewing energy and also shortens the lifetime of the PMMA tooth.

The aim of the paper is to analyze the axial vibration of the artificial PMMA tooth caused by impact and to define the time variable elasticity function of the modified PMMA structure as to eliminate or reduce the vibration.

The research result is suggested to be the basis for programming of the 4D printed modified PMMA tooth. Namely, 4D printing is the technology in which manufacturers can produce materials with self-folding interactions.¹⁶ The 3D printing is extended with the fourth dimension which includes the time variation of the parameter.¹⁷ The prescribed elasticity time variable function, would be incorporated into concept of microstructure of the 3D printed material. Although the 4D printing procedure is equal to that in 3D process through computer-programmed deposition of material in successive layers, in the 4D printing in PMMA the so called "smart" or "programmable" material would be included. The elasticity variation in PMMA would be activated only due to action of the external chewing force. The input from the 3D printed item would become another structure *via* the impact of external energy source. Thus, the 4D printing would have the capacity to alter shape over time and to eliminate the axial vibration.

ANALYTIC PROCEDURE FOR DYNAMIC ANALYSIS OF THE 3D PRINTED PMMA TOOTH MODEL

For dynamic analysis the 3D printing PMMA tooth is modeled as a clamped-free rod with circle cross-section and length which is approximately equal to diameter. The impact force, which lasts for a short time τ and acts along the rod, causes axial vibration.

Model of the 3D printed PMMA tooth

Due to chewing, the force which acts on the tooth causes axial vibration. The aim of the paper is to consider the effect of the impact force on the tooth made of PMMA material.

The shape of the tooth is designed as a clamped-free (fixed at one end and free at the other) short circular rod (Fig. 1). Three types of models are considered: one, of barrel type (Fig. 1a), the second, of cylindrical type (Fig. 1b) and the third is of hollow type (Fig. 1c).

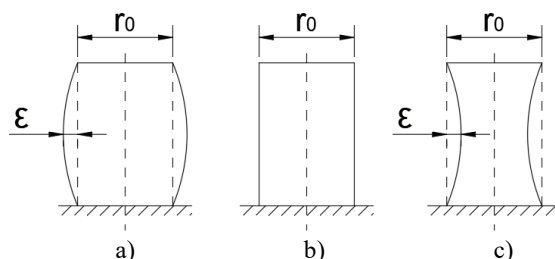


Fig. 1. Models of tooth: a) barrel type model ($\varepsilon > 0$), b) constant cylindrical model ($\varepsilon = 0$), c) concave model ($\varepsilon < 0$).

For the first and third model the cross-section is varying along the rod axis and the radius function $r(x)$ is:

$$r(x) = r_0 \pm \varepsilon \left(\sin \frac{\pi x}{l} \right) \quad (1)$$

where r_0 is the initial radius, $\varepsilon \ll 1$ is the small perturbation value, l is the length of the model, x is the axial coordinate, sign + is for the barrel type model in Fig. 1a and sign - is for concave model in Fig. 1c. For the cylindrical model (Fig. 1b) the radius is constant and $\varepsilon = 0$, i.e., $r = r_0 = \text{const}$.

Remark. In the following text the Eq. (1) with sign + is considered.

Let us consider the equilibrium of the elementary part of the rod. The element has the mass dm and the high is dx (Fig. 2). The element is in equilibrium if the following equation is satisfied:

$$\frac{\partial}{\partial t} \left(dm \frac{\partial u}{\partial t} \right) + F = F + \frac{\partial F}{\partial x} dx \quad (2)$$

where F is the force which acts in axial direction, u is the deflection and t is time.

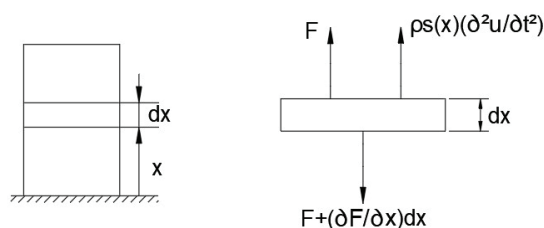


Fig. 2. Equilibrium of an elementary section of the model.

The axial force is the product of the stress σ and the cross section S :

$$F = S(x)\sigma \quad (3)$$

where $S(x) = r^2(x)\pi$. The stress-strain rheological model is assumed to be of linear Kelvin-Voigt type:

$$\sigma = E \frac{\partial u}{\partial x} + \frac{\partial}{\partial t} \left(b \frac{\partial u}{\partial x} \right) \quad (4)$$

where E is the Young's modulus of elasticity and b is the parameter of the deformation velocity. Analyzing the experimentally obtained elasticity values it is obtained that it is varying slowly in time. So, the parameter b is described as a function of "slow time" τ , *i.e.*, $b = b(\tau)$ where $\tau = \nu t$ and $\nu \ll 1$ is a small parameter. Substituting Eq. (3) with Eq. (4) into Eq. (2) it is obtained:

$$\frac{\partial}{\partial t} \left(\rho S(x) \frac{\partial u}{\partial t} \right) = \frac{\partial}{\partial x} \left(ES(x) \frac{\partial u}{\partial x} + S(x) \frac{\partial}{\partial t} \left(b(\tau) \frac{\partial u}{\partial x} \right) \right) \quad (5)$$

The relation (5) is the mathematical expression of the vibration model. It is a linear partial differential equation with time and coordinate variable parameters. For the boundary conditions:

$$u(0,t) = 0, \quad \frac{\partial u}{\partial x}(l,t) = 0 \quad (6)$$

the solution of Eq. (5) is assumed in the form:

$$u(x,t) = T(\tau) \sin \left(\frac{\pi x}{2l} \right) \quad (7)$$

Substituting Eq. (7) into Eq. (5) it is obtained:

$$\begin{aligned} S(x) \ddot{T} \sin \left(\frac{\pi x}{2l} \right) + (\omega^2 T + \frac{b(\tau)}{\rho} \dot{T}) [S(x) \left(\frac{\pi}{2l} \right)^2 \sin \left(\frac{\pi x}{2l} \right) - \frac{\partial S(x)}{\partial x} \left(\frac{\pi}{2l} \right) \cos \left(\frac{\pi x}{2l} \right)] = \\ = -T \frac{1}{\rho} \frac{\partial b(\tau)}{\partial t} [S(x) \left(\frac{\pi}{2l} \right)^2 \sin \left(\frac{\pi x}{2l} \right) - \frac{\partial S(x)}{\partial x} \left(\frac{\pi}{2l} \right) \cos \left(\frac{\pi x}{2l} \right)] \end{aligned} \quad (8)$$

Averaging the periodic functions over the length of the rod l :

$$\begin{aligned} \frac{1}{l} \int_0^l S(x) \sin \left(\frac{\pi x}{2l} \right) dx = \frac{1}{l} \int_0^l (r_0^2 \pi \sin \left(\frac{\pi x}{2l} \right) + 2\varepsilon_0 r_0 \pi \sin \left(\frac{\pi x}{l} \right) \sin \left(\frac{\pi x}{2l} \right)) dx = 2r_0^2 + \frac{8}{3} \varepsilon_0 r_0 \\ \frac{1}{l} \int_0^l \left(\frac{\partial S(x)}{\partial x} \cos \left(\frac{\pi x}{2l} \right) \right) dx = 4\varepsilon_0 r_0 \pi \frac{\pi}{2l} \cos \left(\frac{\pi x}{l} \right) \cos \left(\frac{\pi x}{2l} \right) = \frac{8}{3} \varepsilon_0 r_0 \frac{\pi}{2l} \end{aligned} \quad (9)$$

and using Eq. (8) after some modification it follows:

$$\left(1 + \frac{4\varepsilon}{3r_0} \right) \ddot{T} + \left(\frac{\pi}{2l} \right)^2 (\omega^2 T + \frac{b(\tau)}{\rho} \dot{T}) = T \frac{1}{\rho} \frac{\partial b(\tau)}{\partial t} \left(\frac{\pi x}{2l} \right)^2 \quad (10)$$

where $\omega^2 = E/\rho$. Using the series expansion for small parameter $\varepsilon/r_0 \ll 1$ and neglecting the terms higher than $O((\varepsilon/r_0)^2)$, the Eq. (10) is:

$$\ddot{T} + \frac{\varepsilon_1 b(\tau)}{\rho} \dot{T} + \omega_1^2 T = -\nu \frac{\varepsilon_1}{\rho} \frac{\partial b(\tau)}{\partial t} T \quad (11)$$

where $\varepsilon_1 = (\pi/2l)^2 (1 - (4\varepsilon/(3r_0)))$ and $\omega_1^2 = \varepsilon_1 \omega^2$. The relation (11) is a second order ordinary differential equation with slow time variable parameters. Unfortunately, to find the exact solution for Eq. (11) is impossible. The approximate method based on time variable amplitude and phase is applied.¹⁸ For $\nu = 0$ and $\tau = 0$ the relation (11) transforms into the equation with constant parameter:

$$\ddot{T} + \frac{\varepsilon_1 b_0}{\rho} \dot{T} + \omega_1^2 T = 0 \quad (12)$$

where $b(0) = b_0$. Solution of Eq. (12) is:

$$T = A \exp(-\delta t) \cos(\Omega t + \theta) \quad (13)$$

where A and θ are arbitrary amplitude and phase, and:

$$\delta = \frac{\varepsilon_1 b_0}{2\rho}, \quad \Omega = \sqrt{\omega_1^2 - \left(\frac{\varepsilon_1 b_0}{2\rho}\right)^2} \quad (14)$$

Comparing Eqs. (11) and (12) it is seen that Eq. (11) is the perturbed version of Eq. (12). According to this conclusion the solution of Eq. (11) is assumed in the form:

$$T = A \exp\left(-\int \delta(\tau) dt\right) \cos \psi \quad (15)$$

and time derivative:

$$\dot{T} = -A\delta \exp\left(-\int \delta(\tau) dt\right) \cos \psi - A\Omega \exp\left(-\int \delta(\tau) dt\right) \sin \psi \quad (16)$$

where $A = A(t)$, $\theta = \theta(t)$, and:

$$\dot{\psi} = \Omega(\tau) + \dot{\theta} \quad (17)$$

$$\delta(\tau) = \frac{\varepsilon_1 b(\tau)}{2\rho}, \quad \Omega(\tau) = \sqrt{\omega_1^2 - \left(\frac{\varepsilon_1 b(\tau)}{2\rho}\right)^2} \quad (18)$$

Comparing the time derivative of Eq. (15) with the assumed one (see Eq. (16)) the constraint follows as:

$$\dot{A} \cos \psi - A \dot{\theta} \sin \psi = 0 \quad (19)$$

Substituting the time derivative of Eq. (16) and the relations (15) and (16) into Eq. (11) it yields:

$$-\dot{A}(\delta \cos \psi + \Omega \sin \psi) + A\dot{\theta}(\delta \sin \psi + \Omega \cos \psi) = Av \left(\left(\frac{\partial \delta(\tau)}{\partial t} - \frac{\varepsilon_1 b(\tau)}{\rho} \right) \cos \psi + \frac{\partial \Omega(\tau)}{\partial t} \sin \psi \right) \quad (20)$$

By rewriting Eqs. (19) and (20) we obtain:

$$\dot{A} = -\frac{1}{\Omega} \left(\left(\frac{\partial \delta(\tau)}{\partial t} - \frac{\varepsilon_1}{\rho} \frac{\partial b(\tau)}{\partial \tau} \right) \cos \psi + \frac{\partial \Omega(\tau)}{\partial t} \sin \psi \right) Av \sin \psi \quad (21)$$

$$\dot{\theta} A = -\frac{1}{\Omega} \left(\left(\frac{\partial \delta(\tau)}{\partial t} - \frac{\varepsilon_1}{\rho} \frac{\partial b(\tau)}{\partial \tau} \right) \cos \psi + \frac{\partial \Omega(\tau)}{\partial t} \sin \psi \right) Av \cos \psi \quad (22)$$

It is at this point the averaging of periodical function ψ is introduced. The averaged equations are:

$$\dot{A} = -\frac{Av}{2\Omega} \frac{\partial \Omega(\tau)}{\partial t} \quad (23)$$

$$\dot{\theta} = -\frac{v}{2\Omega} \left(\frac{\partial \delta(\tau)}{\partial t} - \frac{\varepsilon_1}{\rho} \frac{\partial b(\tau)}{\partial \tau} \right) \quad (24)$$

Integrating Eq. (23) for the initial condition $A(0) = A_0$ the amplitude variation is:

$$A = A_0 \sqrt{\frac{\Omega}{\Omega(\tau)}} \quad (25)$$

Substituting Eq. (25) into Eq. (24) it is:

$$\dot{\theta} = \frac{\nu}{4\Omega} \frac{\varepsilon_1}{\rho} \frac{\partial b(\tau)}{\partial \tau} \quad (26)$$

Finally, the averaged solution of Eq. (15) is:

$$T = A_0 \sqrt{\frac{\Omega}{\Omega(\tau)}} \exp\left(-\int \frac{\varepsilon_1 b(\tau)}{2\rho} dt\right) \cos\left(\theta_0 + \int \left(\sqrt{\omega_1^2 - \left(\frac{\varepsilon_1 b(\tau)}{2\rho}\right)^2} + \frac{\nu}{4\Omega} \frac{\varepsilon_1}{\rho} \frac{\partial b(\tau)}{\partial \tau}\right) dt\right) \quad (27)$$

where $\theta(0) = \theta_0$. After some simplification the approximate solution is:

$$T = A_0 \sqrt{\frac{\Omega}{\Omega(\tau)}} \exp\left(-\int \frac{\varepsilon_1 b(\tau)}{2\rho} dt\right) \cos\left(\theta_0 + \Omega t + \frac{\varepsilon_1 (b(\tau) - b_0)}{4\Omega\rho}\right) \quad (28)$$

Finally, in general, the vibration is:

$$u = \sum_{n=1}^{\infty} A_{0n} \sqrt{\frac{\Omega}{\Omega(\tau)}} \exp\left(-\int \frac{\varepsilon_1 b(\tau)}{2\rho} dt\right) \cos\left(\theta_{0n} + \Omega t + \frac{\varepsilon_1 (b(\tau) - b_0)}{4\Omega\rho}\right) \sin\left(\frac{n\pi x}{2l}\right) \quad (29)$$

where A_{0n} and θ_{0n} satisfy the initial conditions. For initial conditions:

$$u(0, x) = P, \quad \frac{\partial u(0, x)}{\partial t} = 0 \quad (30)$$

where P is the chewing force which causes the vibration, the amplitude A_0 and the first term of Eq. (29), u_1 , follows as:

$$A_0 = P \left(1 + \left(\frac{\delta}{\Omega}\right)^2\right), \quad \tan \theta_0 = \frac{\delta}{\Omega} \quad (31)$$

$$u_1 = P \left(1 + \left(\frac{\delta}{\Omega}\right)^2\right) \sqrt{\frac{\Omega}{\Omega(\tau)}} \exp\left(-\int \frac{\varepsilon_1 b(\tau)}{2\rho} dt\right) \cos\left(\tan^{-1}\left(\frac{\delta}{\Omega}\right) + \Omega t + \frac{\varepsilon_1 (b(\tau) - b_0)}{4\Omega\rho}\right) \sin\left(\frac{\pi x}{2l}\right) \quad (32)$$

Vibration in the tooth depends on the initial shape of the tooth (parameter ε) and on the material property ($b(\tau)$ function). For the decreasing slow time function ($b(\tau)$ vibration is of damping type, Eq. (32)). The energy dissipation is faster for faster decrease of $b(\tau)$. Namely, in Eq. (32) both terms:

$$\sqrt{\frac{\Omega}{\Omega(\tau)}} \quad \text{and} \quad \exp\left(-\int \frac{\varepsilon_1 b(\tau)}{2\rho} dt\right)$$

have the same tendency: if $b(\tau)$ increases, the both terms increase and also their product.

RESULTS AND DISCUSSION

Let us assume the model, with modified PMMA material, with slow time elasticity variation:

$$b(\tau) = \frac{b_0}{1 + \tau} \quad (33)$$

The Eq. (32) transforms into:

$$u_1 = P \left(1 + \left(\frac{\delta}{\Omega}\right)^2\right) \left(\frac{\omega_1^2 - \delta^2}{\omega_1^2 - \delta^2 / (1 + \tau)^2}\right)^{1/4} (1 + \tau)^{-\delta/\nu} \times \cos\left(\tan^{-1}\left(\frac{\delta}{\Omega}\right) + \Omega t + \frac{\delta}{2\Omega} \frac{1}{1 + \tau}\right) \sin\left(\frac{\pi x}{2l}\right) \quad (34)$$

For numerical data: $\omega = 1.18 \times 10^9 \text{ s}^{-1}$, $b_0 = 10^3 \text{ N s m}^{-2}$, $\rho = 1170 \text{ kg m}^{-3}$, $E = 223 \text{ MPa}$, $\nu = 0.1 \text{ s}^{-1}$, the temporal vibration expression (28) is treated as:

$$T = A_0 \left(\frac{\omega_1^2 - \delta^2}{\omega_1^2 - \delta^2 / (1 + \tau)^2}\right)^{1/4} (1 + \tau)^{-\delta/\nu} \cos\left(\tan^{-1}\left(\frac{\delta}{\Omega}\right) + \Omega t + \frac{\delta}{2\Omega} \frac{1}{1 + \tau}\right) \quad (35)$$

In Fig. 3 the axial vibrations of the upper surface of three tooth models (Fig. 1) are plotted: $\mu = 0$ is the model with constant circular cross-section, $\mu = 0.5$ is the parameter of barrel type (convex) model, $\mu = -0.1$ is of the concave model, where $\mu = 4\varepsilon/3r_0$. In Fig. 3 it is seen that for all three models the amplitude of vibration has the tendency of decrease. The velocity of vibration amplitude decrease is faster for the concave than for the convex model and even for that with constant cross-section. The period of vibration is also shorter for the concave model than for the model with constant radius and for the convex model.

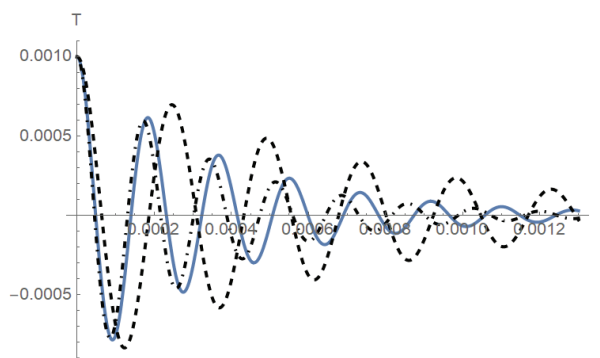


Fig. 3. Temporal time function for various values of parameter μ : $\mu = 0$ (full line), $\mu = 0.5$ (dashed line), $\mu = -0.1$ (dash-dot line).

To determine the total time necessary for vibration delimitation it is necessary to know that the chewing rate varies in the interval 0.94–2.5 chewings/s.¹⁹ Namely, vibration elimination has to be finished in the maximal time interval between two chewings which is approximately 0.4 seconds. It is obvious from the Fig. 2 that the 4D printed model, made of PMMA material with stored energy and programmed according to Eq. (33), is able to eliminate the vibration in the corresponding time interval.

In Fig. 4 the influence of the modulus of elasticity E on the vibration properties is tested. For $\mu = 0$ and modulus of elasticity is $E = 1190$ MPa and $E = 2084$ MPa the temporal function is plotted. It is obtained that the elasticity value has the influence on the frequency of vibration, but the influence on the amplitude vibration is not significant. For higher is the value of the modulus E , the period of vibration is shorter.

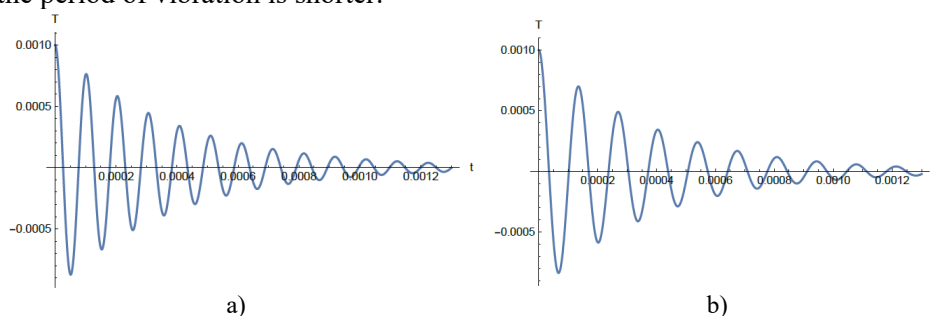


Fig. 4. Axial vibration for various elasticity modulus: a) $E = 1190$ MPa, b) $E = 2084$ MPa.

In Fig. 5 the influence of parameter ν on vibration properties of the model are considered. The parameter values are $\nu = 0$ and $\nu = 1$. It is obtained that for higher value of parameter ν the amplitude of vibration is higher, The influence of ν on the period of vibration is negligible.

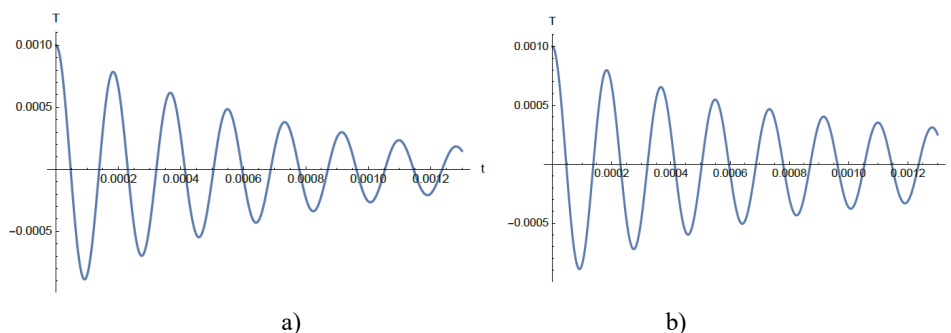


Fig. 5. Temporal time function for various values of ν : a) $\nu = 0$, b) $\nu = 1$ s⁻¹.

In Fig. 6 the $T-t$ diagrams for $b_0 = 10^3$ N s m⁻² and $b_0 = 500$ N s m⁻² are plotted. It is obtained that for higher value of the parameter b_0 the velocity of amplitude decay is slower than for smaller parameter value. The parameter b_0 has the influence on the frequency of vibration.

CONCLUSIONS

It is concluded:

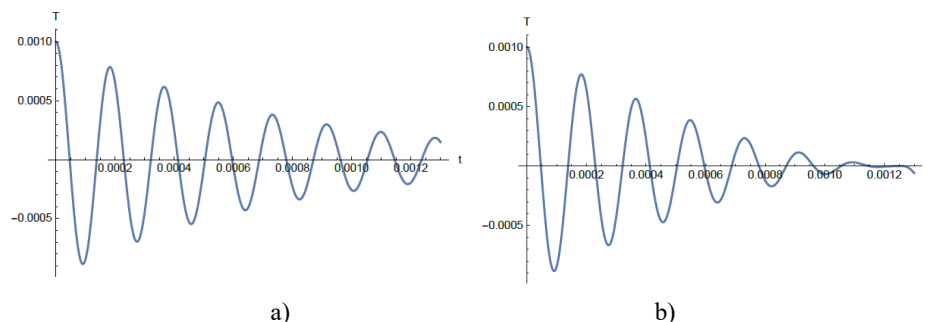


Fig. 6. The $T-t$ diagrams for avariable b_0 a) $b_0 = 10^3 \text{ N s m}^{-2}$; $b_0 = 500 \text{ N s m}^{-2}$.

1. Impact force in chewing causes axial vibration of the 3D printed PMMA elastic tooth.

2. Vibration of the tooth depends on the tooth shape. The vibration amplitude and phase variation is more intensive for barrel formed tooth than for the tooth with constant circular cross section and is the smallest for the tooth of concave form. Namely, the tooth with concave form behaves like the unit in auxetic structure. The deformation and vibration along the axial axis for this 3D printed PMMA model is smaller than for the model with constant cross section and is suggested to be applied in the 4D printing of the tooth,

3. Decay of axial vibration is obtained by using the PMMA modified material with slow time variable elastic property. Damping of vibration is more intensive if the elasticity of the modified PMMA material is decreasing in time.

4. The elasticity property of 3D printed PMMA tooth has the influence on the frequency of axial vibration: the higher is the value of modulus of elasticity, the period of vibration is shorter.

5. Based on the axial vibration time function, the elasticity variation of the 3D printed PMMA material is prescribed. In the tooth, designed with this elasticity – slow time function, elimination or reduction of the axial vibration is expected.

Future research has to be oriented toward 4D printing of PMMA tooth where a new material assembly (a combination of multiple materials, for example) has to be created under stress that becomes “stored” within the material. This stress can later be released, causing an overall material shape change according to elasticity variation as suggested in the result of the paper. To realize tooth, with time variable elastic function, the PMMA has to be modified to be the smart material. It would be the programmable matter, wherein after the fabrication process, the printed tooth reacts with force parameters within the environment and changes its form accordingly.

Acknowledgement. We have to thank Dr Miljan Sunjevic for his help in preparing the Graphical Abstract and Figures.

ИЗВОД

УТИЦАЈ ВАРИЈАЦИЈЕ ЕЛАСТИЧНОСТИ 3Д ШТАМПАНЕ ПММА СТРУКТУРЕ НА АКСИЈАЛНЕ ВИБРАЦИЈЕ ЗУБА

ЛИВИЈА ЦВЕТИЋАНИН^{1,2}, МИЉАНА ПРИЦА¹ и САЊА ВУЈКОВ³

¹Универзитет у Новом Сагу, Факултет техничких наука, Нови Сад, ²Obuda University, Budapest, Hungary и ³Универзитет у Новом Сагу, Медицински факултет, Департаман за стоматологију, Нови Сад

Од недавно, 3Д штампање са поли метил метакрилатом (РММА) има широку примену у стоматологији: 3Д штампа је погодна метода за производњу било ког сложеног тродимензионалног облика, а РММА је материјал који има погодна својства у окружењу усне шупљине. Због тога се 3Д штампа веома често примењује за израду РММА зуба. Ови зуби у току жвакања долазе у контакт, јавља се између њих удар који доводи до промене облика и вибрације зуба. Како цикличне вибрације лоше утичу на издржљивост РММА зуба, оне се морају елиминисати. Циљ овог рада је проучавање аксијалних вибрација 3Д штампаног зуба као и давање препорука за модификацију структуре РММА са циљем пригушивања вибрација. Вибрације зуба су математички моделоване и аналитички решене. Добијени резултат даје везу између вибрационих својстава и варијације еластичности РММА материјала. Функција која дефинише промену еластичности РММА зависи од „спорог времена“. (Израз „споро време“ подразумева производ времена и параметра који је мањи од један). За опадајућу функцију еластичности, вибрација је пригушена: што је интензивније смањење еластичности, то је брже опадање вибрација. На основу утврђене функције еластичности може се реализовати модификација структуре РММА. Аутори предлажу примену добијене функције варијације еластичности за програмирање 4Д штампе са модификованим РММА.

(Примљено 18. јануара, ревидирано 15. фебруара, прихваћено 7. марта 2024)

REFERENCES

1. T. K. Vaidyanathan, J. Vaidyanathan, D. Arghavani, *Acta Biomater. Odontol. Scand.* **2** (2016) 108 (<http://dx.doi.org/10.1080/23337931.2016.1219664>)
2. G. Oberoi, S. Nitsch, M. Edelmayer, K. Janjic, A. S. Müller, H. Agis, *Front. Bioeng. Biotechnol.* **6** (2018) 172 (<http://dx.doi.org/10.3389/fbioe.2018.00172>)
3. H. Cai, X. Xu, X. Lu, M. Zhao, Q. Jia, H.-B., Jiang, J.-S. Kwon, *Polymers* **15** (2023) 2405 (<https://doi.org/10.3390/polym15102405>)
4. L. Peñate, J. Basilio, M. Roig, M. Mercadé, *J. Prosthet. Dent.* **114** (2015) 248 (<https://doi.org/10.1016/j.prosdent.2014.12.023>)
5. A. Nulty, *Clin. Dent.* **2** (2022) 44 (<http://doi.org/10.20944/preprints202105.0316.v1>)
6. M. S. Zafar, *Polymers* **12** (2020) 2299 (<http://dx.doi.org/10.3390/polym12102299>)
7. R. Q. Frazer, R. T. Byron, P. B. Osborne, K. P. West, *J. Long-Term Eff. Med. Implant* **15** (2005) 629 (<http://doi.org/10.1615/jlongtermeffmedimplants.v15.i6.60>)
8. S. M. Pituru, M. Greabu, A. Totan, M. Imre, M. Pantea, T. Spinu, A. M. C. Tancu, N. O. Popoviciu, I.-I. Stanescu, E. Ionescu, *Materials* **13** (2020) 2894 (<http://dx.doi.org/10.3390/ma13132894>)
9. S. Jain, M. E. Sayed, M. Shetty, S. M. Alqahtani, M. H. D. Al Wadei, S. G. Gupta, A. A. A. Othman, A. H. Alshehri, H. Alqarni, A. H.; Mobarki, *Polymers* **14** (2022) 2691 (<https://doi.org/10.3390/polym14132691>)

10. G. Alp, S. Murat, B. Yilmaz, *J. Prosthodont.* **28** (2018) e491 (<http://doi.org/10.1111/jopr.12755>)
11. M. Petras, O. Naka, S. Doukoudakis, A. Pissiotis, *J Esthet Restor Dent* **24** (2012) 26 (<http://doi:10.1111/j.1708-8240.2011.00467.x>)
12. C. Polzin, S. Spath, H. Seitz, *Rapid Prototyp. J.* **19** (2013) 37 (<http://dx.doi.org/10.1108/13552541311292718>)
13. P. Protopapa, E. Kontonasaki, D. Bikiaris, K. M. Paraskevopoulos, P. Koidis, *Dent. Mater. J.* **30** (2011) 222 (<http://dx.doi.org/10.4012/dmj.2010-135>)
14. K. Afaf, B. Serier, K. Kaddouri, M. Belhouari, *Fratt. Ed. Integrità Strutt.* **53** (2020) 66 (<http://dx.doi.org/10.3221/IGF-ESIS.53.06>)
15. M. Wieckiewicz, V. Opitz, G. Richter, K. W. Boening, *Biomed Res. Int.* **2014** (2014) 150298 (<http://dx.doi.org/10.1155/2014/150298>)
16. H. Hamza, *Innovation* **1** (2018) e17 (<http://dx.doi.org/10.30771/2018.4>)
17. M. Javaid, A. Haleem, R. P. Singh, S. Rab, R. Suman, L. Kumar, *J. Oral Biol. Craniofac. Res.* **12** (2022) 388 (<https://doi.org/10.1016/j.jobcr.2022.05.002>)
18. L. Cveticanin, *Strong Nonlinear Oscillators – Analytical Solutions, Mathematical Engineering*, 2nd ed., Springer, Berlin, 2018 (ISBN 978-3-319-58825-4)
19. M. Farooq, E. Sazonov, *Electronics (Basel)* **5** (2016) (<https://doi.org.10.3390/electronics5040062>).